Neuron
Article

The Transcription Factor Pax6 Regulates Survival of Dopaminergic Olfactory Bulb Neurons via Crystallin αA

Jovica Ninkovic,[1,2] Luisa Pinto,[1,6] Stefania Petricca,[1] Alexandra Lepier,[2] Jian Sun,[3] Michael A. Rieger,[1,7] Timm Schroeder,[1] Ales Cvekl,[3] Jack Favor,[4] and Magdalena Götz[1,2,5,*]
[1]Helmholtz Zentrum München, Institute of Stem Cell Research, Ingolstädter Landstraße 1, D-85764 Neuherberg, Germany
[2]Institute of Physiology, Department of Physiological Genomics, Ludwig-Maximilians University Munich, Schillerstrasse 46, 80633 Munich, Germany
[3]Department of Ophthalmology and Visual Sciences and Genetics, Albert Einstein College of Medicine, Bronx, NY 10461, USA
[4]Helmholtz Zentrum München, Institute of Human Genetics, Ingolstädter Landstraße 1, D-85764 Neuherberg, Germany
[5]Munich Center for Integrated Protein Science CiPS[M], Munich, Germany
[6]Present address: Life and Health Sciences Research Institute, School of Health Sciences, University of Minho, Braga, Portugal
[7]Present address: Georg-Speyer-Haus, Institute for Biomedical Research, Paul-Ehrlich-Strasse 42–44, 60596 Frankfurt am Main, Germany
*Correspondence: magdalena.goetz@helmholtz-muenchen.de
DOI 10.1016/j.neuron.2010.09.030

SUMMARY

Most neurons in the adult mammalian brain survive for the entire life of an individual. However, it is not known which transcriptional pathways regulate this survival in a healthy brain. Here, we identify a pathway regulating neuronal survival in a highly subtype-specific manner. We show that the transcription factor Pax6 expressed in dopaminergic neurons of the olfactory bulb regulates the survival of these neurons by directly controlling the expression of crystallin αA (CryαA), which blocks apoptosis by inhibition of procaspase-3 activation. Re-expression of CryαA fully rescues survival of Pax6-deficient dopaminergic interneurons in vivo and knockdown of CryαA by shRNA in wild-type mice reduces the number of dopaminergic OB interneurons. Strikingly, Pax6 utilizes different DNA-binding domains for its well-known role in fate specification and this role of regulating the survival of specific neuronal subtypes in the mature, healthy brain.

INTRODUCTION

Despite their well characterized role in development, functions of homeobox transcription factors in the adult brain still remain elusive. For example, members of the paired-type homeobox (Pax) transcription factor family are expressed in specific neurons in the midbrain and the olfactory bulb (Stoykova and Gruss, 1994), but neither their targets nor the physiological role of this late expression is known. As almost all Pax transcription factors act as fate determinants during development (Osumi et al., 2008), it is possible that they function similarly in adulthood to maintain neuronal identity. Alternatively, Pax transcription factors expressed in mature neurons may regulate novel targets important for specification or regulation of neuronal function and activity. Finally, it is conceivable that Pax transcription factors regulate pathways involved in neuronal survival. Indeed, it is puzzling that specific types of neurons succumb to neurodegeneration, despite the rather widespread expression of the genes affected by the disease-causing mutations (Alavian et al., 2008; Friedlander, 2003; Zhao et al., 2008). Thus, neuronal subtype-specific expression of regulatory transcription factors may contribute to selective cell death.

Here, we examined the role of Pax6 in mature dopaminergic neurons of the olfactory bulb (OB) in mice. Pax6 is expressed in stem and progenitor cells in some regions of the developing CNS during neurogenesis (Ericson et al., 1997; Heins et al., 2002; Kohwi et al., 2005; Stoykova and Gruss, 1994; Stoykova et al., 2000) but only in very few neuronal subpopulations in the adult brain, such as the dopaminergic neurons in the glomerular layer of the OB, granule neurons in the cerebellum, and amacrine and ganglion cells of the retina (Stoykova and Gruss, 1994). Pax6 expression in progenitors ceases at early postnatal stages and persists only in progenitors in the adult neurogenic regions (Brill et al., 2009; Hack et al., 2005; Kohwi et al., 2005; Stoykova and Gruss, 1994). Pax6 acts proneurogenic in adult neural progenitors (Hack et al., 2005), similar to its role during development (Heins et al., 2002), but also plays a role to specify neuronal subtype identity in the adult and developing brain (Hack et al., 2005; Kohwi et al., 2005; Kroll and O'Leary, 2005; Nikoletopoulou et al., 2007; Stoykova et al., 2000; Tuoc et al., 2009). Pax6 cooperates with Dlx2 in adult neuroblasts to specify the dopaminergic identity of periglomerular neurons (PGNs) in the olfactory bulb (Brill et al., 2008; Hack et al., 2005). As only these dopaminergic neurons continue to express Pax6 lifelong, it is also conceivable that Pax6 may be further required to maintain this neuronal subtype identity. Interestingly, the dopamine levels are subject to activity dependant regulation in PGNs (Bastien-Dionne et al., 2010).

Here, we used genetic ablation of Pax6 exclusively in mature dopaminergic neurons and found that Pax6 is essential to inhibit programmed cell death of these neurons by controlling the expression of CryαA which prevents activation of procaspase-3. These data reveal a pathway of transcriptional regulation of

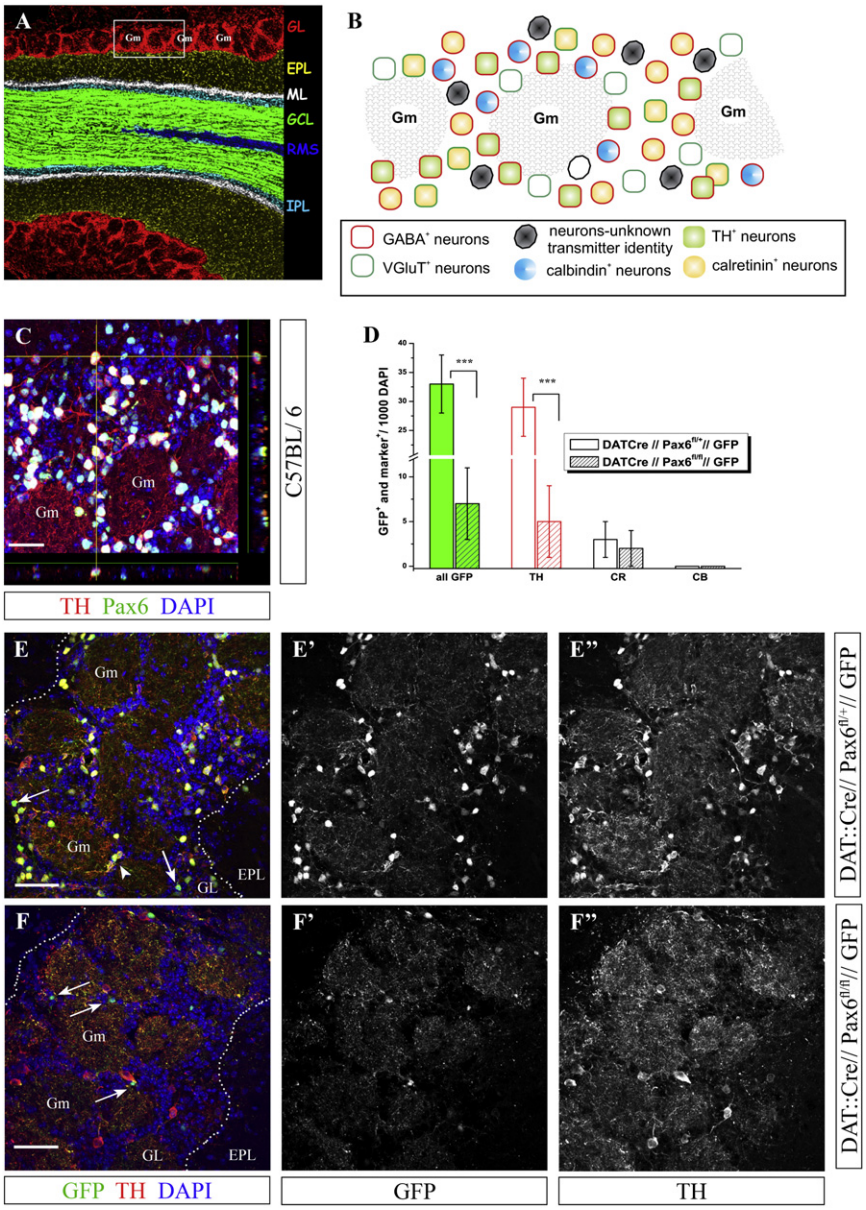

Figure 1. Pax6 Function Is Necessary for the Survival of Dopaminergic Periglomerular Neurons

(A and B) Schematic representation of the main neuronal layers in the OB (A) and neuronal subtypes in the GL (B, region depicted as white square in A).

(C) Fluorescence micrograph depicting that virtually all TH-immunoreactive dopaminergic periglomerular neurons (red) also contain Pax6 (green) in 3-month-old mice.

(D–F) Loss of Pax6 in homozygous $Pax6^{fl/fl}$ mice after DAT::Cre mediated recombination and indicated by GFP reporter (green) results in reduced reporter$^+$ (D, E′, F′) and TH$^+$ (red) (D, E″, F″) cells (11 animals for control and 7 for $Pax6^{fl/fl}$). (E and F) Fluorescence micrographs depicting the GL (outlined with dotted lines) of Pax6 deficient animals (F) and heterozygote siblings (E) immunostained for TH (red) and GFP reporter (green). Note the reduced number of cells positive for the GFP reporter (indicating Pax6-deficient cells) and for TH in $Pax6^{fl/fl}$ animal (arrows in (F).

Abbreviations: GL, glomerular layer; EPL, external plexiform layer; ML, mitral cells; GCL, granular cell layer; RMS, rostral migratory stream; IPL, internal plexiform layer; Gm, glomerulus; TH, tyrosine hydroxylase; CR, calretinin; CB, calbindin. Scale bars: 50 μm. ***$p < 0.001$ and brackets in (D) represent SEM. See also Figure S1.

neuronal survival in a highly subtype-specific manner in the adult brain.

RESULTS

Pax6 Is Necessary for Survival of Dopaminergic PGNs

Periglomerular neurons (PGNs) represent a heterogeneous population of both excitatory and inhibitory interneurons in the olfactory bulb (Figures 1A and 1B; Brill et al., 2009; Kosaka et al., 1988; Kosaka and Kosaka, 2007; Nakamura et al., 2005). A subpopulation of about 20% of the inhibitory PGNs employs the transmitter dopamine and expresses the transcription factor Pax6 (Figure 1C). Consistent with previous data (Hack et al., 2005), we found that virtually all dopaminergic PGNs identified as immunoreactive to the dopamine transporter (DAT), which is expressed only in fully mature dopaminergic neurons several weeks after their birth (Revay et al., 1996), are also Pax6 immunoreactive (91% ± 3%, n[animals] = 11, at least 1000 cells per animal analyzed). Similarly neurons expressing tyrosine hydroxylase (TH), the rate-limiting enzyme for dopamine biosynthesis, in the glomerular layer are positive for Pax6 (Figure 1C).

To address the function of Pax6 in these fully mature postmitotic neurons we genetically ablated Pax6 by Cre-Lox recombination in mice with Cre expressed from the DAT locus (DAT::Cre [Zhuang et al., 2005]) and exons 4–6 of the Pax6 gene flanked by loxP sites ($Pax6^{fl/fl}$) (Ashery-Padan et al., 2000). Since Pax6 is not expressed in any other dopaminergic neuron population in the brain (Stoykova and Gruss, 1994), this allowed us to specifically examine the role of Pax6 in dopaminergic OB interneurons. Recombination mediated by DAT::Cre and indicated by a GFP reporter (Novak et al., 2000) was specific to mature DAT-expressing neurons (no DAT-negative cells were recombined and GFP$^+$ [see Figures S1A and S1B available online]) and efficient (70% ± 6% of all DAT$^+$ PGNs were GFP$^+$; 5 animals; 450 cells analyzed per animal; Figures S1A and S1B). Notably, however, we also observed a small fraction of calretinin$^+$ PGNs expressing DAT and hence also being

recombined by DAT::Cre (Figure S1F), while no overlap was found with calbindin$^+$ PGNs (Figure S1H).

We were surprised to see that Cre$^+$ cells in 2-month-old DAT::Cre//Pax6$^{fl/fl}$ mice were still Pax6 immunoreactive (Figure S1E). To examine whether this is due to a failure to recombine the Pax6 floxed alleles or to stability of the Pax6 protein, we examined Pax6 mRNA in the GFP$^+$ PGNs isolated by FACS. We observed that Pax6 mRNA levels were severely decreased in GFP$^+$ PGNs of DAT::Cre//Pax6$^{fl/fl}$ mice to 10% ± 3% of its level in their DAT::Cre//Pax6$^{fl/+}$ siblings, while Pax6 protein levels were not yet reduced, suggesting a high stability of Pax6 protein in postmitotic neurons. When we examined DAT::Cre// Pax6$^{fl/fl}$ mice at 3.5 months of age, virtually all Cre$^+$ PGNs had lost Pax6 protein (Figures S1C, S1D, and S1E).

After Pax6 had disappeared, we noted a profound reduction in GFP$^+$ and TH$^+$ or DAT$^+$ neuron numbers in the OB (Figures 1D–1F). This decrease in the number of dopaminergic PGNs may result from a fate conversion upon loss of Pax6, as Pax6 acts as a fate determinant of the dopaminergic PGN subtype throughout adulthood (Brill et al., 2008; Hack et al., 2005). However, we saw neither an increase in any other neuronal subtypes (calretinin$^+$ or calbindin$^+$) in the GL of DAT::Cre//GFP//Pax6$^{fl/fl}$ mice in comparison to their WT siblings (Figures 1D and S1F–S1I), nor reporter positive cells immunoreactive for typical glial markers such as GFAP, S100β, O4, or GST-π (data not shown) in the OBs of DAT::Cre//GFP//Pax6$^{fl/fl}$. Moreover, no other abnormalities were detectable in the OBs of DAT::Cre//GFP//Pax6$^{fl/fl}$ mice (Figures S1J–S1P), suggesting that neither fate conversion nor non-cell-autonomous effects took place after Pax6 deletion in dopaminergic PGNs. Instead, we observed a significant decrease in the number of GFP reporter$^+$ cells in the OBs of DAT::Cre//GFP//Pax6$^{fl/fl}$ compared to heterozygous or WT littermate mice (Figure 1D), suggesting that the dopaminergic neurons may succumb to cell death rather than acquire a different fate. This loss of dopaminergic PGNs was not due to unspecific effects of expressing high levels of Cre or GFP in dopaminergic neurons, as DAT::Cre//GFP$^+$ neurons did not die in the OB of heterozygous floxed mice nor in the midbrain where Pax6 is not expressed in the dopaminergic neurons (data not shown). Therefore, these data suggest that loss of Pax6 affects specifically the survival of mature dopaminergic PGNs.

To elucidate the mechanism by which Pax6-deficient neurons die, we stained dissociated cells of the adult OB for propidium iodide (PI) and annexinV (Casciola-Rosen et al., 1996) to discriminate live (annexinV-negative, PI-negative), early apoptotic (annexinV-positive, PI-negative) and necrotic/late apoptotic (annexinV-positive, PI-positive) cells (Figures 2A and 2B). Reporter-positive (Figure 2C), Pax6$^{fl/fl}$ cells from the OB of 3.5 month old mice contained significantly ($p < 0.01$) more early apoptotic cells (21.1% ± 1.5%; 3 animals, 10,000 events per animal) than cells from the OB of their heterozygous siblings (13.2% ± 1.0%; 3 animals, 10000 events per animal) (Figures 2D and 2E) that did not differ from WT animals (data not shown). Among adult generated neuroblasts that newly arrive in the OB, about 50% succumb to cell death and the remainder incorporate into the neuronal network (Petreanu and Alvarez-Buylla, 2002). Several thousand new neurons, including dopaminergic neurons, arrive per day in the OB (Lois and Alvarez-Buylla, 1994), which explains the high proportion of cells in the early apoptotic phase among GFP$^+$ cells in the OB of WT and heterozygous Pax6$^{fl/+}$ mice. Also, there was no difference in annexinV-positive nonrecombined reporter negative cells (data not shown), supporting the specificity and cell-autonomous nature of apoptosis induced in dopaminergic OB neurons upon loss of Pax6. To further assay for apoptotic death of dopaminergic PGNs in these mice we performed activated caspase-3 immunostaining. We observed a significant 3-fold increase ($p < 0.05$) in the number of activated caspase-3 immunoreactive cells among the Pax6-deficient dopaminergic neurons at 3 months of age (Figure 2F), the time when Pax6 immunoreactivity is lost in the OB dopaminergic neurons (Figure S1E).

Loss of CryαA Expression Causes Neuronal Death upon Pax6 Depletion

To further elucidate the role of Pax6 in preventing programmed cell death (PCD) in dopaminergic PGNs, we examined the pathways that commit dopaminergic PGNs to the PCD in the absence of Pax6 function. p75 and galectin have been implicated in regulating neuronal cell death (Nikoletopoulou et al., 2007; Plachta et al., 2007), including the death of misspecified neurons in the embryonic cortex and midbrain (Alavian et al., 2009; Nikoletopoulou et al., 2007; Plachta et al., 2007). We examined p75 and galectin in the adult OB upon loss of Pax6. The number of cells immunoreactive for p75 and galectin (Figures S2A–S2C and data not shown) and the mRNA expression levels of p75 (Figure S2D) among the reporter positive cells isolated by FACS did not differ between the genotypes. As this analysis was carried out at the stage when the annexinV$^+$ fraction of dopaminergic OB neurons was increased (3.5-month-old mice; Figures 2D and 2E), we concluded that p75 and galectin are not altered and not responsible for the death of dopaminergic PGNs devoid of Pax6.

Next, we examined the crystallin gene family (Lanneau et al., 2008) since its members are well-known targets of Pax6 in the lens (Cvekl and Duncan, 2007) and also regulate cell survival (Morozov and Wawrousek, 2006). Among the crystallins, αB- and βB2-crystallin have been reported to be expressed in the brain (Graw, 2009). However, in neurons of the OB including dopaminergic PGNs, we surprisingly detected crystallin αA (CryαA), which had not yet been reported to be expressed in the brain (Graw, 2009; Figures 3A, 3B, and S3). Interestingly, CryαA expression was confined to the mature neurons immunoreactive to the panneuronal marker NeuN (Figures S3C–S3E). While 97% of DAT::Cre$^+$ cells were CryαA$^+$ in WT and heterozygous Pax6$^{fl/+}$ mice (704 cells counted, 6 animals), only 20% (820 cells counted, 9 animals) were double positive in Pax6$^{fl/fl}$ mice at 3.5 months of age (Figures 3B and 3C), demonstrating a specific loss of CryαA in the Pax6-deficient neurons. These data raised the possibility that the reduced levels of CryαA may be causative for the death of dopaminergic PGNs after loss of Pax6.

To test this hypothesis, we transduced adult neuronal progenitors in the RMS of 2.5-month-old mice with lentiviruses encoding for CryαA-specific shRNA 5 (Figures 3E, S4A, and S4B) or for a control shRNA (Figure 3D). Both virus constructs expressed GFP from an independent promoter to identify transduced cells. As CryαA shRNA 5 efficiently knocks down CryαA (Figures S4A and S4B), we depleted CryαA from all adult-generated OB

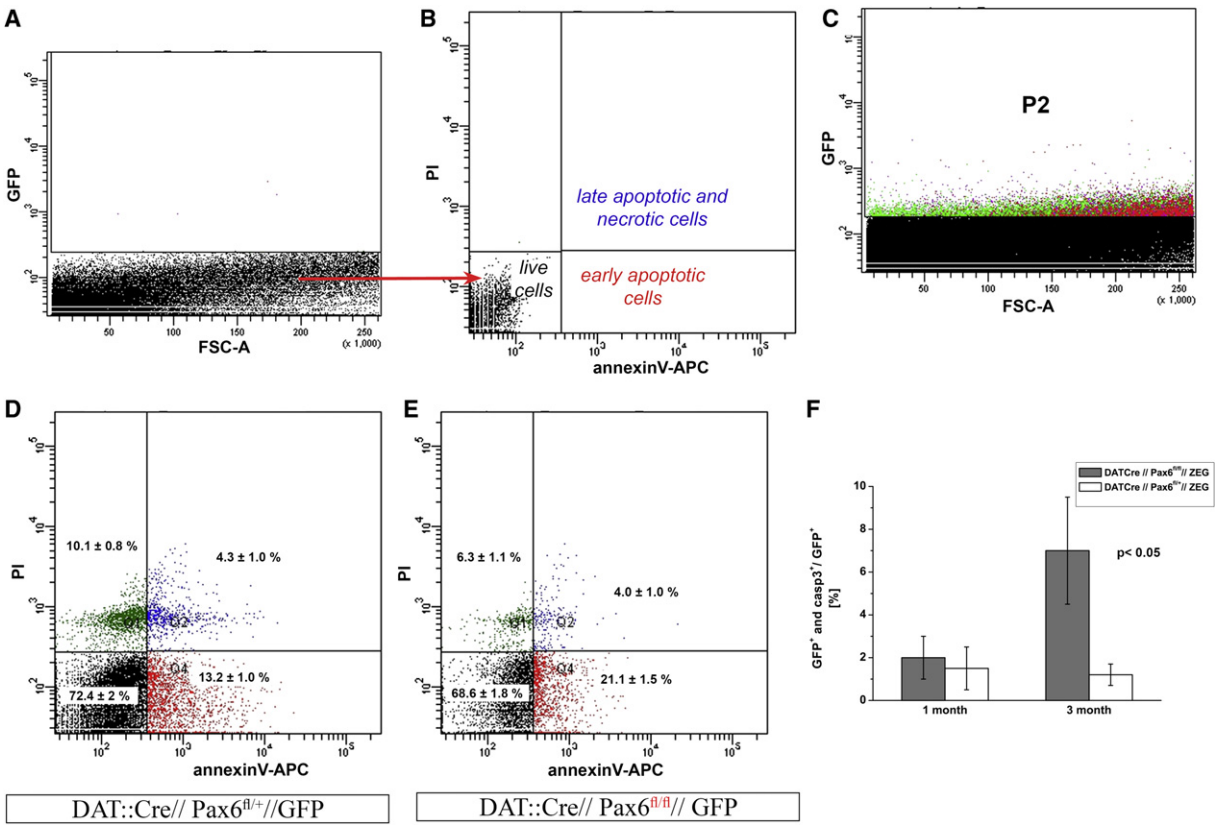

Figure 2. Propidium Iodide (PI)/AnnexinV-Based Cell Death Analysis of OB Cells after DAT::Cre-Mediated Pax6 Deletion

This method is based on the difference in integrity of the plasma membrane in apoptosis and necrosis. One of the earliest features of apoptotic cells is the translocation of the phospholipid phosphatidylserine (PS) from the inner to the outer leaflet of the plasma membrane. Therefore, early apoptotic cells can be efficiently labeled with annexinV, which has a high affinity to PS. Loss of plasma membrane integrity, characterizing both necrosis and the late phase of apoptosis, allows passage of propidium iodide (PI) through the plasma membrane and labeling of DNA. Assessing recombined, reporter positive cells (P2) population in (C) in the DAT::Cre//GFP//Pax6$^{fl/fl}$ (E) and DAT::Cre//GFP//Pax6$^{fl/+}$ control animals (D) for PI and annexinV, allowed us to distinguish between live (annexinV-negative, PI-negative), early apoptotic (annexinV-positive, PI-negative) and necrotic/late apoptotic (annexinV-positive, PI-positive) cells (B).

(A and B) Dot blots illustrating gate definition for the GFP (A), PI, and annexinV (B) based on analysis of WT (GFP-negative) not stained cells.

(C–E) Dot blots showing the analyses of recombined cells (P2 population) in Pax6 mutant (DAT::Cre//GFP//Pax6$^{fl/fl}$) (E) and its control sibling (D).

(F) Histogram depicting the proportion of recombined cells immunoreactive to activated caspase-3 before (1 month) and after (3 month) the loss of Pax6 protein (three animals analyzed per genotype, per time point and at least 150 cells analyzed per animal). Data are shown as mean value ± SEM.

See also Figure S2.

neurons. Despite CryαA knockdown, neuronal differentiation was not changed 8 weeks after viral vector injection, and we could not observe any differences in the distribution of GFP-positive cells in the OB between control and CryαA shRNA transduced cells (Figure 3F). However, when we analyzed the proportion of transduced cells with dopaminergic identity 8 weeks after the viral transduction, we observed a significant decrease ($p < 0.005$) in DAT$^+$ cells among transduced cells to 25% of the proportion observed in the control shRNA transduced cells (Figure 3F). Thus, CryαA is specifically required for the survival of dopaminergic, but not of all adult generated OB interneurons.

To test whether CryαA is sufficient to maintain dopaminergic neurons even in the absence of Pax6, we examined whether CryαA expression rescues Pax6-deficient dopaminergic PGNs from apoptosis. We infected adult neuronal progenitors migrating in the rostral migratory stream toward the OB with a MLV-based retroviral vector encoding for CryαA and dsRed or a control vector containing dsRed only (Figures 3G and 3H). Thereby we target all adult generated neuroblasts with a permanent, Pax6-independent expression of CryαA. To allow sufficient differentiation time and to examine whether migration and differentiation occurs normally despite the overexpression of CryαA, we examined the OBs 2 months after viral vector injection into the RMS of 2.5-month-old DAT::Cre//GFP//Pax6$^{fl/+}$ or DAT::Cre//GFP//Pax6$^{fl/fl}$ mice. Virus-transduced (dsRed$^+$; white arrow in Figures 3G and 3H) cells had reached the OB and differentiated into dopaminergic neurons (yellow arrow in Figure 3H). These dopaminergic neurons also expressed DAT::Cre and were GFP$^+$ (Figures 3D–3F). The proportion of dopaminergic neurons labeled by GFP (in green) among the virally transduced cells expressing dsRed (in red) in DAT::Cre//GFP//Pax6$^{fl/+}$ mice was similar to previous analyses (Brill et al., 2008; Hack et al., 2005) and did not differ between virus expressing CryαA and control virus expressing only dsRed (Figure 3I). These data indicate that overexpression of CryαA

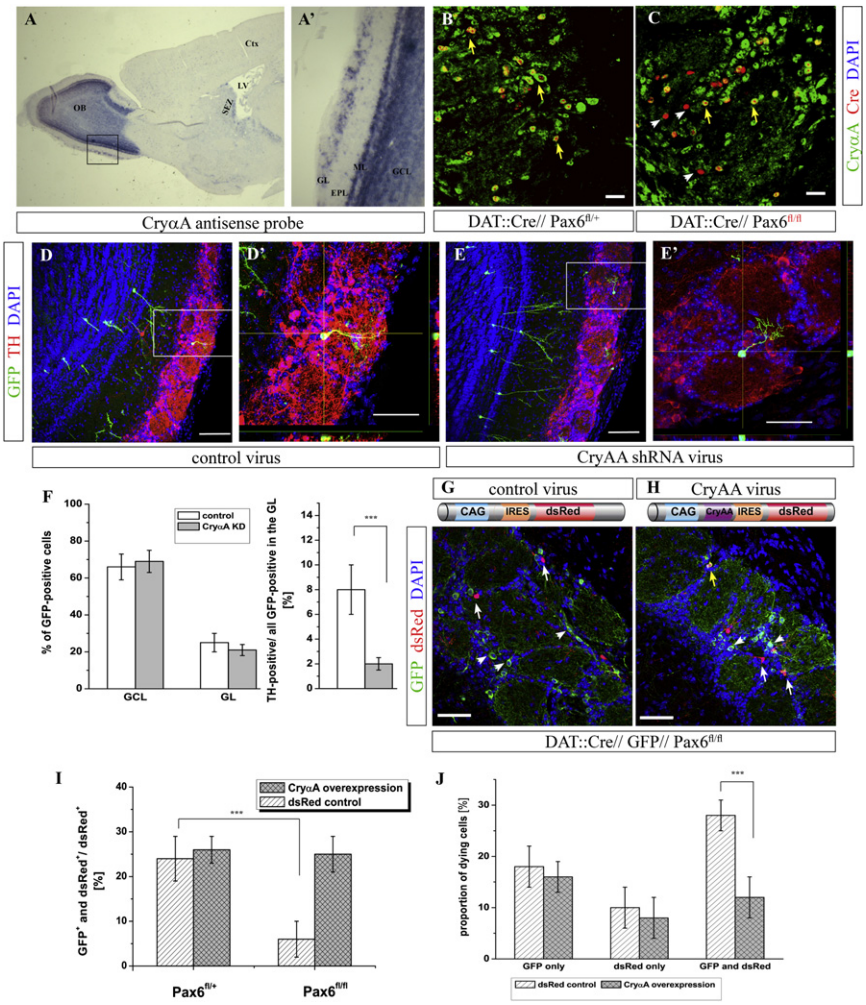

Figure 3. CryαA Is Sufficient to Rescue the Survival of Pax6-Ablated Periglomerular Neurons

(A and A′) Micrographs depicting CryαA mRNA expression in the adult brain confined to the OB.

(B and C) Micrographs depicting the reduced proportion of Cre$^+$ (red) cells double-labeled for CryαA (green; yellow arrows indicate double$^+$ cells) after loss of Pax6 in DAT::Cre//GFP//Pax6$^{fl/fl}$ mice (C, 20% ± 4% double$^+$; 9 animals) compared to the control (B, 97% ± 3% double$^+$; 6 animals).

(D–E) Micrographs depicting dopaminergic neuronal population in the olfactory bulb (TH, red) after lentivirus-mediated CryαA knockdown (E and E′) and overexpression of the control shRNA (D and D′). Transduced cells are GFP-immunoreactive and (D′) and (E′) are magnifications of boxed areas in (D) and (E), respectively.

(F) Histograms showing the distribution of CryαA (gray bars) or control shRNA (open bars) transduced cells in the OB 8 weeks after transduction (left histogram) and the proportion of dopaminergic neurons (right histogram). Note significant decrease ($p < 0.005$) in CryαA-deficient cells with dopaminergic identity (2% ± 0.5% of all transduced cells in the GL, 4 animals analyzed), compared with the control shRNA transduced cells (8% ± 2% of all transduced cells in the GL, 4 animals analyzed).

(G–J) Retrovirus-mediated CryαA expression (red in H and I) rescues the loss of dopaminergic PGNs (green as GFP$^+$ by DAT::Cre//GFP; yellow arrow) in DAT::Cre//GFP//Pax6$^{fl/fl}$ mice (three animals), while control virus expressing DsRed only (G and I) fails to rescue (three animals). (J) Histogram depicting the annexinV-positive, dying cells 6 weeks after the re-expression of CryαA (GFP and dsRed) or control vector (dsRed only) in the Pax6-depleted periglomerular neurons identified by the GFP immunoreactivity (three animals analyzed).

Abbreviations: as in Figure 1 and Ctx, cortex; LV, lateral ventricle; SEZ, subependymal zone; OB, olfactory bulb. Scale bars: 20 μm in (B) and (C); 50 μm in (D), (E), (G), and (H) and 100 μm in (D′) and (E′). ***$p < 0.001$ and brackets in (F) and (I) are SEM.

See also Figure S3.

does not interfere with migration and differentiation of the infected cells. Moreover, the proportion of dopaminergic GFP$^+$ neurons is equal between cells overexpressing CryαA and cells infected with the control virus in the OB of DAT::Cre//GFP//Pax6$^{fl/+}$ mice (Figure 3I), suggesting that endogenous levels of CryαA are sufficient for maximal survival. Conversely, in DAT::Cre//GFP//Pax6$^{fl/fl}$ the proportion of dopaminergic GFP$^+$ neurons among the control dsRed$^+$-labeled cells was reduced to less than 20% of control levels (Figure 3I) demonstrating that the survival of adult generated dopaminergic PGNs depends on the maintenance of Pax6 expression in their mature state. In pronounced contrast, the proportion of GFP$^+$ dopaminergic neurons among the CryαA transduced cells was equal to the controls even in DAT::Cre//GFP//Pax6$^{fl/fl}$ (Figures 3E and 3F), demonstrating that CryαA expression is able to fully rescue the dopaminergic neurons upon loss of Pax6 protein. Notably, this rescue also demonstrated that these cells do not need Pax6 expression per se to maintain their dopaminergic identity, as deletion of Pax6 in mature DAT-expressing neurons did not alter the proportion of this neuronal subtype when its survival was rescued by CryαA expression.

To determine whether CryαA re-expression in Pax6-deficient dopaminergic PGNs rescues their numbers due to improved survival, we analyzed the proportion of dying cells using the annexinV-based assay in DAT::Cre//GFP//Pax6$^{fl/fl}$ animals with or without CryαA-mediated rescue by FACS. We observed a 2-fold decrease in the proportion of dying cells after retroviral vector expression of CryαA compared to the control vector (Figure 3J; cells double-positive for dsRed and GFP). Importantly, the overexpression of CryαA did not affect the survival of nondopaminergic cells that had a similar rate of 10% cell death in both CryαA and control virus-transduced cells (Figure 3J; dsRed only cells) in agreement with no change in the number of nondopaminergic cells upon retroviral expression of CryαA (Figures 3G–3I). Taken together, CryαA does not alter the fate and the specification of PGN but prevents PCD of dopaminergic PGNs downstream of Pax6.

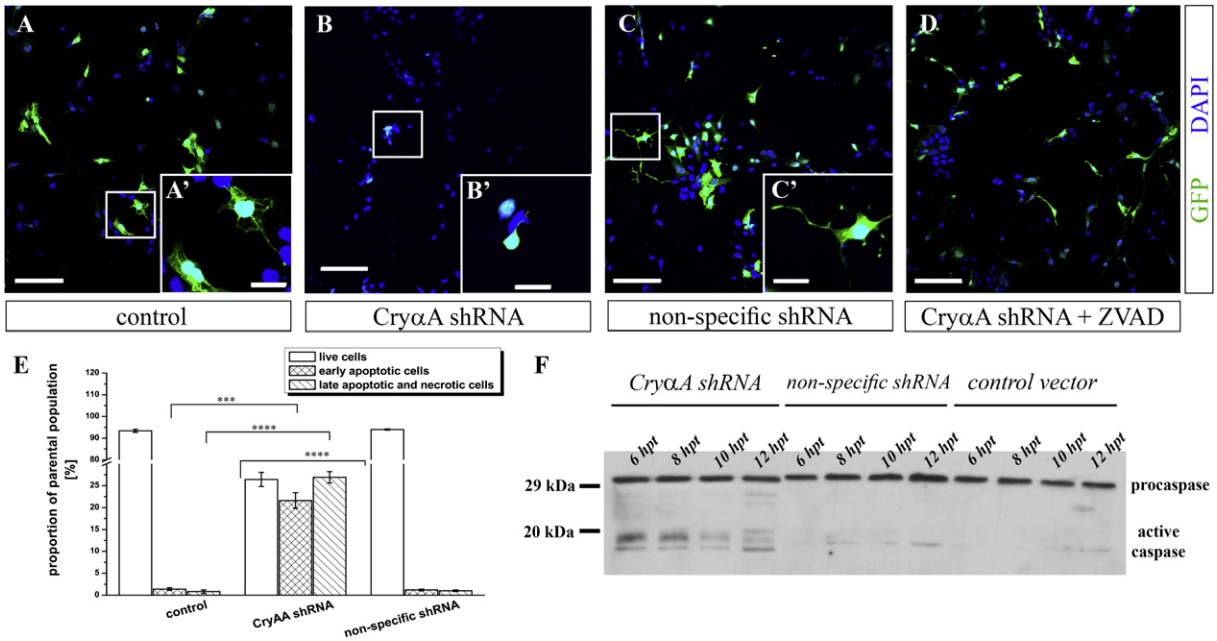

Figure 4. CryαA Knockdown Induces Apoptosis via Caspase-3 Activation

(A–C) Confocal images showing reduction in numbers of P19 cells transfected with the virus expressing GFP and CryαA-specific shRNA5 (B and B′) compared to the controls (A, A′, C, and C′).

(D) Caspase specific inhibitor ZVAD-fmk blocks the effect of CryαA-specific shRNA5 on number and morphology of P19 cells (compare D and B).

(E) Histogram depicting the increase in the proportion of early apoptotic and late apoptotic/necrotic cells after CryαA knockdown as detected by annexinV and PI staining and FACS analyses (3 experiments, 10,000 events per condition).

(F) Western blot depicting the activation of procaspase-3 (upper band, 30 kDa) and release of active caspase-3 form (lower bands, 13 and 17 kDa) only after the transient transfection of P19 cells with CryαA specific shRNA5.

Abbreviations: hpt, hours after transfection; ***$p < 0.001$; ****$p < 0.0001$. Brackets in (E) are SEM. Scale bars: 50 μm in (A), (B), (C) and (D); 10 μm in (A′), (B′) and (C′). See also Figure S4.

CryαA Prevents Activation of Caspase-3

We performed shRNA mediated knockdown of CryαA in the P19 cell line grown under both undifferentiated and differentiated conditions (see Experimental Procedures). P19 cells express Pax6 and CryαA in both conditions investigated (Figures S4B and S5C) and the CryαA protein can be efficiently depleted from these cells by CryαA-specific shRNA5 expression as described above (Figures S4A and S4B). Supporting the idea that a reduction of CryαA results in apoptosis, shRNA5-mediated CryαA knockdown in P19 cells resulted in reduced numbers of CryαA-shRNA5-transfected cells compared to the control shRNAs (Figures 4A–4C) by 30 hr after the transfection. CryαA shRNA5-expressing cells display cell rounding, pyknotic nuclei and nuclear fragmentation (Figure 4 and data not shown), the typical hallmarks of cells undergoing PCD (Boldyrev, 2000). Significantly increased fractions of early apoptotic and late apoptotic/ necrotic cells preceded the reduction in the number of CryαA-shRNA5 transduced cells, as revealed by PI and annexinV staining 24 hr after transduction (Figure 4E). As the activation of caspase-3 is the key event in the commitment of cells to PCD (Conradt, 2009), we examined caspase-3 protein following CryαA knockdown. When protein extract from control or CryαA-shRNA5 transduced P19 cells was probed with an anti-caspase antibody recognizing both active (13 and 17 kDa) and pro-form (39 kDa), only cells exposed to CryαA knockdown showed activated caspase-3 (Figure 4F). Conversely, these bands were undetectable after control transfection or in the protein extracts of nontransfected cells (Figure 4F). Consistent with a role of caspase-3 activation in mediating the CryαA knockdown triggered apoptosis, treatment of CryαA shRNA5-transfected cells with the caspase inhibitor ZVAD-fmk fully abolished cell death (Figure 4D). As activation of caspase-3 has also been implicated in cellular functions other than PCD, such as neuronal differentiation (Chen et al., 1998), we performed time-lapse imaging (Costa et al., 2008; Eilken et al., 2009) to further examine the role of CryαA. Although 90% of the progeny of CryαA-specific shRNA5 transfected cells died within 35 hr of observation (Figures S4C and S4D), CryαA knockdown did not interfere with cell cycle length or the mode of division of P19 cells grown in undifferentiated conditions (Figure S4E), compatible with our in vivo results showing no influence on proliferation, migration and cell fate after viral vector-mediated knockdown or overexpression in vivo. Taken together, these data identify CryαA as a key regulator of the apoptotic pathway in neurons.

Pax6 Homeodomain Controls CryαA Expression

Downregulation of CryαA expression in dopaminergic PGNs after loss of Pax6 suggests that Pax6 may directly control CryαA expression. Pax6 regulates target gene expression by three DNA-binding domains, the paired domain (PD) with the PAI and

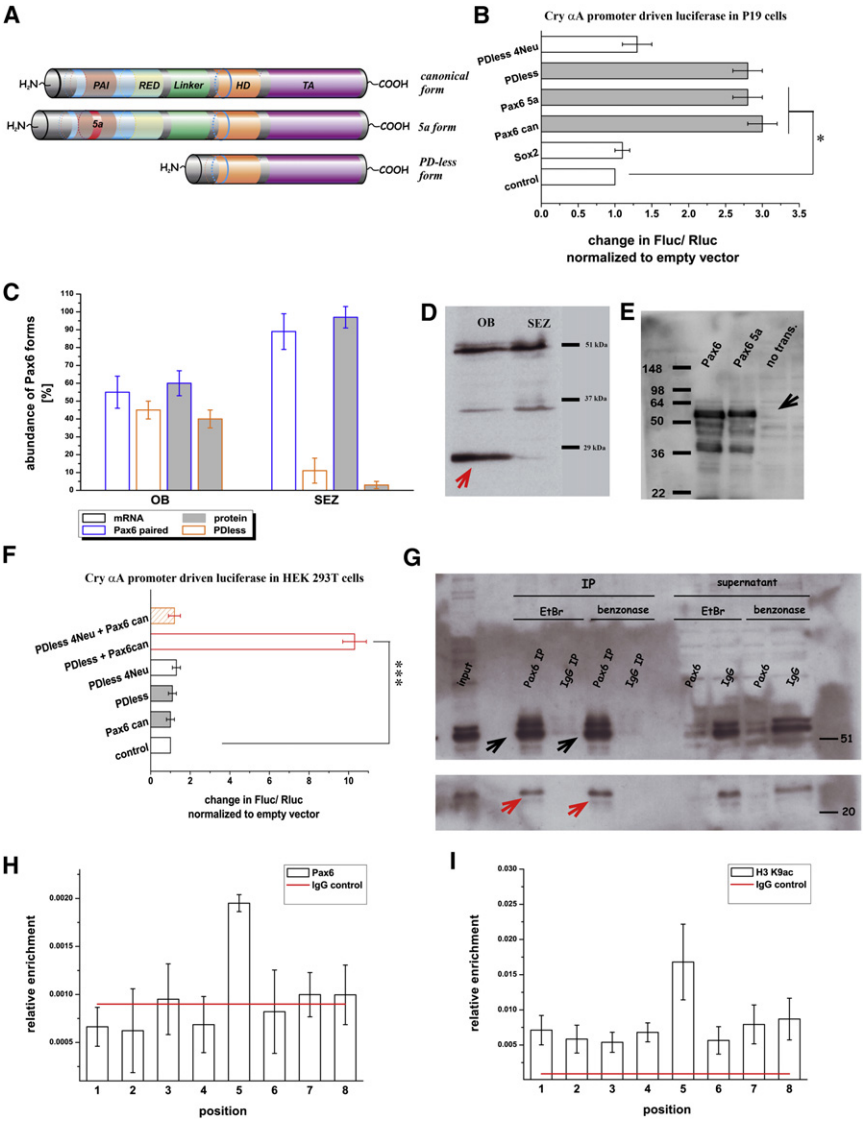

Figure 5. Pax6 Homeodomain Activates CryαA Expression

(A) Scheme depicting different forms of the Pax6 transcription factor (B). The canonical, 5a, and PD-less Pax6 forms activate reporter gene expression driven by the 2.1 kb CryαA promoter (Yang et al., 2006), while introduction of a point mutation interfering with the homeodomain DNA-binding in the PD-less form (blue ring in A) abolishes the reporter activation (five experiments) in the Pax6-expressing P19 cell line.

(C) The relative abundance of different Pax6 forms measured at RNA (qRT-PCR) and protein (western blot) level in the adult OB and SEZ.

(D) Western blot for Pax6 depicting enrichment of PDless Pax6 form (arrow) in the OB compared to the SEZ lysates. Note that both SEZ and OB contain canonical Pax6 and Pax65a (50–55 kD bands).

(E) HEK293T cells do not express any Pax6 forms. Western blot for Pax6 in nontransfected (right line) and HEK293T cells transfected with constructs expressing Pax6 (left line) or Pax65a (middle line) using AB2237 antibody that recognize all Pax6 forms because of C-terminal binding.

(F) In HEK293T cells lacking endogenous Pax6, co-expression of canonical and PD-less forms of Pax6 is necessary to activate 2.1 kb CryαA promoter (Yang et al., 2006) (red bar), while Pax6, Pax65a, and PD-less alone do not activate the reporter construct. Note that the point mutation affecting DNA binding capacity of HD abolished CryαA promoter activation.

(G) PD-less interacts with canonical Pax6 in the OB. Western blot for all Pax6 forms (rabbit anti-Pax6 antibody [see Figure S4]) in immunoprecipitates of canonical Pax6 (immunoprecipitated with the N-terminal Pax6 antibody [see Figure S4]) from total lysates of the adult OB. No signal for Pax6 forms was detected in the wash fraction or immunoprecipitates using IgG control, whereas signals for both canonical (black arrow) and PD-less Pax6 (red arrow) forms were detected after both EtBr and benzonase treatment indicated direct protein-protein interaction in the adult OB between full length Pax6 and PD-less.

(H and I) Histograms depicting Pax6 (H) and H3 K9ac (I) distribution at the mouse αA-crystallin gene locus in OB chromatin. The numbers on x axis represent the primer position in CryαA locus (Yang et al., 2006). The red line indicates median background signal averaged through the CryαA locus. The relative enrichment (RE) unit represents 10% of the input.

*$p < 0.05$; ***$p < 0.001$ and brackets in (B), (C), (F), (H), and (I) are SEM. See also Figure S5.

the RED subdomains and the paired-type homeodomain (HD; Figure 5A). Alternative splicing (Epstein et al., 1994) or different transcription initiation (Glaser et al., 1992) generate mainly three Pax6 forms, the canonical Pax6 containing all three DNA-binding motifs, the Pax6(5a) form in which binding of the PAI domain to DNA is abolished and the PDless form that lacks the entire paired domain (PD-less) and can bind DNA only via its homeodomain (Figure 5A; see also Haubst et al., 2004). To test whether any of these Pax6 proteins would regulate CryαA we examined transcriptional activation of the 2.1 kb CryαA promoter (Yang et al., 2006) in luciferase assays performed in N2A and P19 cells (Figures 5A and 5B). Consistent with previous data obtained with lens cells (Yang et al., 2006), transduction of Pax6 forms containing the PD and HD (canonical and 5a) led to a significant increase in CryαA promoter mediated luciferase expression (Figure 5B). In contrast to the data obtained with lens cells, we also observed activation by the PDless protein (Figures 5A and 5B). DNA binding of this HD is essential for activation of the CryαA promoter as a point mutation abolishing DNA binding of the HD ($Pax6^{4Neu}$) (Favor et al., 2001) also abolished the activation of this promoter (Figure 5B). Taken together, these data suggest that Pax6 directly regulates CryαA expression by DNA binding of the HD.

We next examined the expression of the different forms of Pax6 in the OB in vivo and found expression of the PDless form, which was virtually absent in the subependymal zone, where adult neural progenitor cells and neuroblasts express Pax6 (Brill et al., 2008; Hack et al., 2005). In contrast, canonical

Pax6 form was present in both SEZ and OB (Figures 5C, 5D, and S6J). These data suggest the intriguing concept that mature neurons expressing Pax6 in the OB specifically upregulate the PD-less form of Pax6.

Given the coexistence of canonical and PD-less forms of Pax6 in vivo (Figures 5C and 5D), we further tested the influence of endogenous Pax6 expressed in P19 cells (Figure S5) by using a cell line lacking endogenous Pax6 expression, HEK293T. When we transduced these cells with the canonical or PD-less form of Pax6, no activation of the CryαA promoter was observed (Figure 5F) in striking contrast to the results obtained in the cell line with endogenous Pax6 levels (Figure 5B). However, cotransduction of the canonical and PD-less form of Pax6 resulted in very strong transcriptional activation of the CryαA promoter (Figure 5F), demonstrating the necessity of these forms to interact. This potent activation was fully abolished by cotransduction of the canonical Pax6 with the PD-less homeodomain mutant (PD-less Pax6^{4Neu}) (Figure 5F). These results show that CryαA transcription depends exclusively on the DNA binding activity of the Pax6 HD of the PDless protein, since it cannot be compensated by the nonmutant HD of the canonical Pax6, and requires interaction of the PD-less form with the canonical form of Pax6.

To examine whether the requirement for both the full length and PD-less form of Pax6 depends on a physical interaction of the two proteins, we performed coimmunoprecipitation experiments in protein extracts from the adult OB. To do so we took advantage of an N-terminal Pax6 antibody that does not recognize the PD-less protein lacking the N terminus (Figures S4F and S4G). Precipitation with this antibody should therefore precipitate only Pax6 forms containing a PD (either canonical or 5a). The immunoprecipitates were then probed with a C-terminal Pax6 antibody recognizing all Pax6 forms (Figure S4F). We observed the PDless protein in Western blots (red arrowhead in Figure 5G). As these experiments were performed after treatment with ethidium bromide or benzonase blocking protein DNA interactions, the data suggest a direct protein-protein interaction between the full length and PDless Pax6 proteins (Figure 5G). Taken together with the data obtained in the luciferase experiments, we conclude that CryαA expression is regulated by HD-mediated DNA binding of a complex consisting of the Pax6 full length and PD-less protein. To demonstrate that Pax6 interacts with the CryαA locus in vivo, we isolated chromatin from OBs of 3-month-old animals and performed a series of qChIP analyses (Figure 5H). The enrichment of Pax6 was found in the CryαA promoter region (regions −500 and −250 bp; Figure 3H). In addition, the −500 bp promoter region showed increased signals corresponding to H3 K9 acetylated histones (Figure 3I), a mark localized to the 5′ regions of transcriptionally active genes (Liang et al., 2004). Taken together, these data suggest that Pax6 directly regulates CryαA expression through association with the upstream promoter regions in chromatin of OB cells.

Paired-Type Homeodomain Dysfunction Impairs Survival of Dopaminergic PGNs

The above experiments suggested a critical role of the HD in regulating CryαA expression and hence dopaminergic PGN survival. We tested this in vivo in a mouse line harboring a point mutation in the Pax6 HD abolishing DNA binding, the Pax6$^{132\text{-}14Neu}$ (further named Pax6^{14Neu}) mice (Favor et al., 2008). In contrast to most Pax6 mutants (Favor et al., 2008; Graw et al., 2005; Haubst et al., 2004), Pax6^{14Neu} is not homozygous lethal. Consistent with normal forebrain development in Pax6 mutants with a defective HD (Haubst et al., 2004), adult mice homozygous for the Pax6^{14Neu} allele also do not show gross morphological changes in the forebrain (Figures S6A–S6C). This allowed us to further study both neurogenesis and survival of dopaminergic neurons in these animals. First, we examined the presence and number of adult neural stem cells in the subependymal zone of Pax6^{14Neu} mice by the neurosphere assay. The number of neurospheres generated, their size and their self-renewing capacity did not differ in Pax6^{14Neu} mice compared to their WT siblings (Figures S6D–S6F). Moreover, neurospheres from the Pax^{14Neu} mutants were tripotent and not different from WT cells in regard to the proportion of neurons, oligodendrocytes and astrocytes generated 7 days after withdrawal of growth factors (Figures S6G–S6H).

As the full length form of Pax6 was previously implicated in adult neurogenesis (Hack et al., 2005; Kohwi et al., 2005), we examined neuroblasts in sections by immunostaining for doublecortin (DCX) and by FACS using live staining for PSA-NCAM. Neuroblasts were present in equal numbers and locations in the Pax6$^{14Neu/14Neu}$ mutants and their heterozygote or WT littermates in both read-outs (Figure S6I and data not shown). As the proportion of PSA-NCAM-positive was quantified in the OB, we can further conclude that an equal number of young neurons arrive to the OB of Pax6$^{14Neu/14Neu}$ animals as in their WT siblings (Figure S6I), demonstrating that neurogenesis and neuronal migration are normal in these mutant mice. This is in full agreement with previous work demonstrating that the DNA-binding mutations of the HD of Pax6 do not affect proliferation, neurogenesis, and neuronal migration during development (Haubst et al., 2004).

However, when we examined the composition of PGNs in the glomerular layer of 3.5-month-old Pax6$^{14Neu/14Neu}$ mice, we observed a significant reduction of DAT$^+$ PGNs to 20% of that of control mice (Figures 6B and 6G). All other PGN subtypes were unaffected (Figures 6C–6G). To examine whether this was due to a failure of DAT$^+$ neurons to be generated or to survive, we applied BrdU to label recently generated dopaminergic neurons. The recently (4–6 weeks before) generated DAT$^+$ neurons comprise only 10% ± 3% of all DAT$^+$ PGNs in control mice (3 animals examined and at least 500 cells counted per genotype). In contrast, the vast majority of the few DAT$^+$ neurons present in the OB of homozygous Pax6^{14Neu} mice were all recently generated (80% ± 5% BrdU$^+$), suggesting that in Pax6^{14Neu} mice DAT$^+$ neurons are generated but quickly lost. Taken together, these data strongly suggest that survival of dopaminergic PGNs is severely compromised in Pax6$^{14Neu/14Neu}$ mice.

Consistent with the evidence presented above that the HD of Pax6 is essential to regulate CryαA, we detected a significant reduction in the density of CryαA$^+$ cells in the Pax6$^{14Neu/14Neu}$ selectively in the glomerular layer (Figure 6H) which was due to a strong reduction in the number of DAT and CryαA

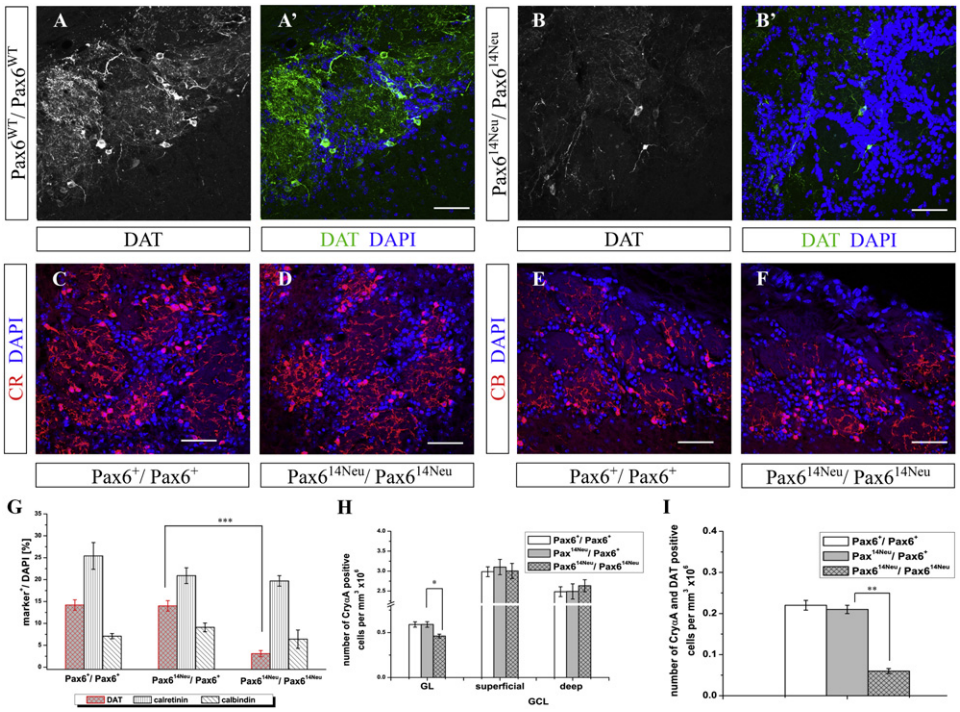

Figure 6. Pax6 Homeodomain Is Necessary for the Maintenance of Dopaminergic OB Interneurons

(A, B, and G) Mature dopaminergic neurons immunoreactive for DAT (green) are significantly decreased in the Pax6^{14Neu} mutant (six animals) deficient for homeodomain function (A and G) compared to the WT (four animals) (B and G) or heterozygous (six animals) siblings (G). The proportion of calretinin and calbindin positive cells did not significantly differ between the mutant and heterozygote or WT animals (G).

(C–F) Micrographs depicting calretinin (C and D) and calbindin (E and F) immunoreactive populations in the OB of Pax6$^{14Neu/14Neu}$ mice (D and F) and their WT siblings (C and E). Note the comparable number of calretinin$^+$ or calbindin$^+$ PGN subtypes in mutant and WT (G). All images are maximum intensity projections of 30 μm optical z stacks.

(H) The density of CryαA-positive cells is significantly reduced in the GL of Pax6^{14Neu} mutants compared to their WT or heterozygous siblings but did not differ in any other OB layer analyzed (three animals analyzed per genotype).

(I) Histogram depicting the reduction in CryαA-positive dopaminergic periglomerular neurons in Pax6^{14Neu} mutants compared to their WT or heterozygous siblings (three animals analyzed per genotype).

Abbreviations: DAT, dopamine transporter; GL, glomerular layer; GCL, granular cell layer; ***$p < 0.001$ and *$p < 0.05$; brackets in (G), (H), and (I) are SEM. Scale bars 50 μm. See also Figure S6.

double-positive cells (Figure 6I; $p < 0.05$, 5 animals per genotype analyzed) compared to their WT or heterozygous siblings. Thus, these data are consistent with the concept that the DNA-binding mutation in the HD of Pax6^{14Neu} causes a downregulation of CryαA in dopaminergic PGNs which results in death of this population. Importantly, no changes in mRNA of either PD or HD containing forms of Pax6 as measured by qPCR were detectable in E14 cortices and adult OBs of Pax6$^{14Neu/14Neu}$ mutants and their age-matched Pax6$^{14Neu/+}$ siblings (Figure S6K and data not shown), supporting the concept that the loss of DAT$^+$ PGNs via loss of CryαA is indeed due to the point mutation in the HD rather than alterations in the overall expression levels of Pax6 that are observed in the full Pax6 mutants and can cause cell death (Holm et al., 2007; Tuoc and Stoykova, 2008).

DISCUSSION

Here, we revealed a function of Pax6 in regulating the survival of specific neuron subtypes in the adult brain. We demonstrated that this function is achieved by utilizing a different DNA-binding domain as used in the developmental functions of Pax6 and is exerted by the regulation of CryαA. CryαA is required to prevent the activation of the caspase cascade and thereby inhibits progression of the dopaminergic OB interneurons to PCD in the adult mouse brain. These results thereby demonstrate a pathway to regulate neuron survival in the adult brain in a subtype-specific manner.

Neuron Survival in the Adult Brain

During development, especially of the peripheral nervous system, PCD is part of the program sculpturing neuron numbers and thereby neuronal connectivity (Dicou and Perez-Polo, 2009). PCD is actively inhibited by external survival cues (Chang and Johnson, 2002) or cell intrinsic mechanisms (Hatzold and Conradt, 2008) regulating different signaling cascades to inhibit the activation of procaspase-3 and thereby promoting the survival of the correct cell types in appropriate numbers (for review see Conradt (2009).

In contrast, little is known about the regulation of neuronal survival in the normal, uninjured adult brain. The number of

neurons in most regions of the adult brain is constant and virtually no neuronal cell death occurs. However, in the regions of the adult brain where neurogenesis continues also PCD continues and only about half of all newly arriving neuroblasts survive (Petreanu and Alvarez-Buylla, 2002). The turnover mode of neurons with replacement of about 10% by newly arriving neurons has been most clearly established in the dentate gyrus (Lagace et al., 2007; Ninkovic et al., 2007) and implies a rather specific regulation of neuronal survival. Notably, the mode of neuron incorporation in the glomerular layer (GL) is very different. Long-term fate mapping of adult generated neurons has revealed a constant increase in their proportion in the GL (Ninkovic et al., 2007), suggesting the addition of new neurons to this network rather than a replacement of preexisting neurons.

Our data now demonstrate mature neurons in the GL require the direct transcriptional orchestration of a survival pathway. We showed that CryαA is expressed in the brain in a highly region-specific manner and acts as an essential survival factor in dopaminergic OB interneurons in the adult mouse brain (Figure 3). CryαA prevents procaspase-3 activation possibly by interaction with Bax and Bcl-Xl as demonstrated in the lens (Mao et al., 2004) or by physical interaction and inhibition of its autocatalytic activation (Kamradt et al., 2001). Moreover, crystallins, as molecular chaperons, interact with the cytoskeleton (Bai et al., 2007) and prevent the deposition of protein aggregates (Bai et al., 2007; Narayanan et al., 2006; Rekas et al., 2004) thereby promoting cell survival (Andley, 2007) in a caspase-independent manner. However, our data are not consistent with the latter mechanisms of CryαA function since cell death by aggregation of proteins would be expected to occur at a slower pace than observed after shRNA-mediated knockdown and the loss of Pax6 and CryαA in the Pax6 mutant OBs. Moreover, our in vitro experiments also support a direct role of CryαA in the regulation of cell survival by influencing procaspase-3 activation. It has been previously shown that deletion of CryαA leads to a decrease in Bad S136 phosphorylation, a potent signal for apoptosis (Xi et al., 2008). In addition, CryαA also interacts with p53 and hence its loss may affect cell death at various levels (Andley, 2007).

One of the most important aspects of this work is the specificity of this pathway affecting exclusively dopaminergic OB interneurons. Knockdown of CryαA in other adult generated neurons did not affect their survival. This is particularly relevant in regard to the alterations of dopaminergic OB interneuron numbers which have been observed in Parkinson's disease patients (Hirsch et al., 1987; Shih et al., 2007; Sulzer, 2007). Interestingly, P19 cells that also depend on CryαA for suppression of caspase-3-dependent cell death are also both GABAergic and dopaminergic (Staines et al., 1994) and express Pax6 as well as CryαA. It may thus be that CryαA is involved in a specific survival pathway active in OB dopaminergic neurons. While we did not observe CryαA expression in midbrain dopaminergic neurons, different members of the crystallin family are expressed in different brain regions and may be implicated in regulating neuronal survival (Ganguly et al., 2008; Magabo et al., 2000; Renkawek et al., 1992). Other homeobox transcription factors could regulate crystallins in other neuronal subtypes, such that this survival pathway may play a general role in specific neurons of the adult brain. The finding that neuronal survival in a healthy adult brain is regulated in a subtype-specific manner is therefore highly relevant to the subtype-specific vulnerability of neurons in many neurodegenerative diseases.

Pax6 Exerts Different Functions via Distinct DNA-Binding Domains

The survival pathway in dopaminergic OB neurons is mediated by the same TF specifying these neurons, but utilizes a different DNA-binding domain, namely the homeodomain. Interestingly, the regulation of CryαA via the HD in the brain is not semidominant as PD-regulated effects of proliferation, neurogenesis, and patterning during development (Ellison-Wright et al., 2004; Estivill-Torrus et al., 2002; Götz et al., 1998; Heins et al., 2002; Kroll and O'Leary, 2005; Stoykova et al., 2000; Toresson et al., 2000; Yun et al., 2001). This is rather different in eye development, where mutations of the HD exhibit strong and early phenotypes (Favor et al., 2001, 2008). Notably, the regulation of crystallins is mediated by the PD in the eye and in lens cells (Chauhan et al., 2002; Cvekl and Duncan, 2007; Cvekl et al., 1994; Wolf et al., 2009), while we show here that it requires the interaction with a full-length and a PDless Pax6 to mediate HD-dependent target regulation.

Lack of Pax6 function can also result in cell death in the developing forebrain (Nikoletopoulou et al., 2007). Interestingly, this cell death is mediated by p75 and occurs as a consequence of misspecification as the misspecified Pax6 mutant GABAergic neurons survive well in other brain regions where GABAergic neurons are normally generated (Nikoletopoulou et al., 2007). In the normal case Pax6-positive progenitors give rise to glutamatergic neurons (Kroll and O'Leary, 2005; Nikoletopoulou et al., 2007; Stoykova et al., 2000). In the absence of Pax6, upregulation of the transcription factors Gsh2, Mash1, and Dlx2 occurs and results in the generation of GABAergic neurons (Kroll and O'Leary, 2005; Schuurmans and Guillemot, 2002; Stoykova et al., 2000; Toresson et al., 2000). When the transient wave of early cell death is rescued by p75 depletion, the misspecified GABAergic neurons survive (Nikoletopoulou et al., 2007). Conversely, rescue of Pax6-deficient dopaminergic OB neurons resulted in the survival of dopaminergic and not other misspecified neuronal subtype. Pax6 expression is transient in the stem and progenitor cells of the developing cerebral cortex and it does not continue in the differentiating glutamatergic neurons in this region (Götz et al., 1998). This further highlights that the cell death of misspecified neurons in the developing cortex is not a direct cause of absence of Pax6 function but depends on the local environment and neuronal misspecification. Conversely, Pax6 exerts a primary role in the regulation of neuronal survival in adult neurons, where it is continuously expressed, by direct regulation of the survival component CryαA that inhibits the apoptosis pathway. Taken together, Pax6 changes its role from PD-mediated transcriptional regulation specifying fate in progenitor cells to HD-mediated transcriptional regulation of cell survival in mature neurons.

EXPERIMENTAL PROCEDURES

Animals

DAT::Cre (Zhuang et al., 2005), Pax6^{fl} (Ashery-Padan et al., 2000), and Z/EG (Novak et al., 2000) were maintained on C57BL6/J background. Animals

were housed in polypropylene cages lined with wood chips. All experimental procedures were performed in accordance with German and European Union guidelines. Stereotactic injections of retroviruses into the brain of adult mice were approved by the Government of Upper Bavaria in license number 211-2531-23/04 and 55.2-1-54-2531-144/07.

Histology and Immunostaining

Immunostainings and analyses were performed as previously described (Brill et al., 2008). Antibodies used: anti-calbindin (Swant, mouse IgG, 1: 200), anti-calretinin (Swant, mouse IgG, 1: 200), anti-Cre (Chemicon, rabbit, 1:200), anti-crystallinαA (Abcam, rabbit, 1:1000), anti-DAT (Abcam, rat, 1:500), anti-dsRed (Chemicon, rabbit, 1:1000), anti-doublecortin (DCX, Chemicon, Guinea pig, 1:1000), anti-GFAP (SIGMA, IgG1, 1:100), anti-GFP (Chemicon, rabbit, 1:5000 or Aves, chicken 1:500), anti-NeuN (Chemicon, IgG1, 1:75), anti-Pax6 (Chemicon, rabbit, 1:700), anti-TH (Chemicon, chick, 1:200), anti-BrdU (rat, 1:200, Abcam) .

In Situ Hybridization

Digoxigenin-labeled RNA probes for CryαA, CryαB, CryβB2, and Cryγ (kindly provided by J. Graw) were made and used as described previously (Brill et al., 2008).

Western Blot

Specific brain areas were dissected and lysed in RIPA buffer containing protease and phosphatase inhibitors (Roche). Ten micrograms of total proteins were separated by 10% SDS-PAGE and transferred to PVDF membranes (Bio-Rad). Membranes were incubated with primary antibodies followed by horseradish peroxidase labeled secondary antibodies (1:25 000; Amersham). These were detected by ECL Western Blotting Detection (Chemicon). The abundance of the band was quantified using ImageJ software after background correction.

Immunoprecipitations

Nuclear extracts were prepared from freshly dissected OBs and dialyzed to 100 mM KCl as described previously (Dignam et al., 1983). For the immunoprecipitation, 10 μg of anti-Pax6 antibody (Hybridoma Developmental Bank) was used for 300 μl of OB nuclear extract

FACS Analysis for Cell Death and Neuroblasts

Olfactory bulbs were dissected and dissociated to single-cell suspension as previously described (Brill et al., 2008). Single-cell suspensions were assessed for cell death using PI/annexinV kit (eBioscience) and FACS analysis according to the manufacturers' recommendations. To assess number of neuroblasts, cells were labeled with mouse anti/PSA-NCAM antibody (Chemicon, 1: 500) for 15 min on ice, followed with Cy-5 conjugated secondary antibody and FACS analyses.

Luciferase Assay

Expression plasmids for luciferase reporter assays were constructed using full-length cDNA of mouse Sox2, Pax6, Pax6(5a), and PDless cloned into the pMXIG vector. The empty vector was used as control. The 2.1 kb CryαA promoter was cloned into the pGL3 vector (Promega). The CryαA promoter was PCR amplified from genomic DNA using the following primers: 5′-TTTATGTATATGAGTACGCTGTTGC and 5′-TCTATTTGGTGATGCAGGGA. We used mouse neuroblastoma (Neuro-2A) and mouse embryonic carcinoma P19 cells (0.5×10^5 cells/ cm^2) and assays we performed according to the manufacturer's instructions (Promega).

Viral Constructs, Virus Production, and Stereotactic Injections

Full-length cDNA of mouse CryαA was cloned into CAG-RFP retroviral vector (cytomegalovirus immediate-early enhancer-chicken β-actin hybrid-red fluorescent protein). An empty CAG-dsRed vector was used as a control. Retrovirus was produced in a packaging cell line (GPG-293) after transient transfection with the retroviral expression plasmid. Estimation of the viral titer was performed as described (Hack et al., 2005) and titered to 5×10^7 colony-forming units (cfu) ml^{-1}. For all experiments, 10-week-old males were stereotactically injected with 1 μl of either CAG-DsRed, CAG-CryαA-DsRed, or shRNA lentiviruses into the left and the right RMS (coordinates relative to the bregma were (in mm): −2.8 anterior/posterior, 0.75 medial/lateral, and −1.9 dorsal/ventral from the dura).

Short-Hairpin RNAs

The short-hairpin RNAs (shRNAs) were designed using BLOCK-iT RNAi Designer (Invitrogen) against the full-length cDNA of CryαA and contain sense, four nucleotides CGAA as the loop, antisense sequences and two adapters for the BglII and HindIII sites. The synthesized double-stranded DNA nucleotides were annealed and ligated into pLVTH plasmids (Wiznerowicz and Trono, 2003) after the H1 promoter. Oligonucleotides designed for CryαA were CryαA_shRNA5: GACTGTTCGACCAGTTCTTCG (21 bp) and CryαA_shRNA6: GTCACCATTCAGCATCCTTGG (21 bp) and nonspecific shRNA: GGTTTGGCA TATAATCTATCG (21 bp). P19 cells were transiently transfected with the shRNA encoding plasmids using Lipofectamine2000 (Invitrogen) according to the manufacturers' specifications and assayed for either cell death or immunocytochemistry as described above.

Chromatin Immunoprecipitation (ChIP) Assays

The qChIP experiments were performed as described (Cuddapah et al., 2009; Lee et al., 2006) with minor modifications. The detailed protocol is available in supplemental material. We used rabbit anti-Pax6 (Millipore/Chemicon, cat # ab2237) or H3K9ac polyclonal antibodies (Abcam, cat #ab4441) for IP.

Quantitative Analysis

Quantifications (proportions of reporter-positive cells among particular cell types) were done using ImageJ software to analyze confocal Z stacks. At least 10 (per animal) corresponding sections were sampled and analyzed at different mediolateral positions and the number of animals is indicated for every experiment. All results are presented as mean and standard error of the mean. Statistical analysis was performed in Microcal Origin 7.5 using ANOVA and Mann-Whitney U test.

SUPPLEMENTAL INFORMATION

Supplemental Information includes six figures, one table, and Supplemental Experimental Procedures and can be found with this article online at doi:10.1016/j.neuron.2010.09.030.

ACKNOWLEDGMENTS

We would like to thank foremost Ruth Ashery-Padan for $Pax6^{fl/fl}$ animals and Jochen Graw for his advice on crystallin function and in situ probes. We thank Yves Barde and Michael Sendtner for their input on the concepts of cell death in the CNS and the analysis of the programmed cell death pathway. We would also like to greatly acknowledge the excellent technical expertise of Andrea Steiner-Mezzadri, Emily Baumgart-Violette, Angelika Waiser, and Detelf Franzen. Many thanks also to Yves Barde, Emily Baumgart-Violette, Benedikt Berninger, and Armen Saghatelyan for great comments on the manuscript. The work was supported by the DFG including the SFB 596 and 870, the BMBF, the Bavarian Ministery for Science and Research (For NeuroCell), the Helmholtz Association (Helma), and the EU (EUTRACC). T.S. was partially supported by the DFG, and A.C. is supported by NIH grants EY012200 and EY014237.

Accepted: August 31, 2010
Published: November 17, 2010

REFERENCES

Alavian, K.N., Scholz, C., and Simon, H.H. (2008). Transcriptional regulation of mesencephalic dopaminergic neurons: the full circle of life and death. Mov. Disord. *23*, 319–328.

Alavian, K.N., Sgadò, P., Alberi, L., Subramaniam, S., and Simon, H.H. (2009). Elevated P75NTR expression causes death of engrailed-deficient midbrain dopaminergic neurons by Erk1/2 suppression. Neural Dev. *4*, 11.

Andley, U.P. (2007). Crystallins in the eye: Function and pathology. Prog. Retin. Eye Res. *26*, 78–98.

Ashery-Padan, R., Marquardt, T., Zhou, X., and Gruss, P. (2000). Pax6 activity in the lens primordium is required for lens formation and for correct placement of a single retina in the eye. Genes Dev. *14*, 2701–2711.

Bai, F., Xi, J.H., and Andley, U.P. (2007). Up-regulation of tau, a brain microtubule-associated protein, in lens cortical fractions of aged alphaA-, alphaB-, and alphaA/B-crystallin knockout mice. Mol. Vis. *13*, 1589–1600.

Bastien-Dionne, P.O., David, L.S., Parent, A., and Saghatelyan, A. (2010). Role of sensory activity on chemospecific populations of interneurons in the adult olfactory bulb. J. Comp. Neurol. *518*, 1847–1861.

Boldyrev, A.A. (2000). Discrimination between apoptosis and necrosis of neurons under oxidative stress. Biochemistry (Mosc.) *65*, 834–842.

Brill, M.S., Snapyan, M., Wohlfrom, H., Ninkovic, J., Jawerka, M., Mastick, G.S., Ashery-Padan, R., Saghatelyan, A., Berninger, B., and Götz, M. (2008). A dlx2- and pax6-dependent transcriptional code for periglomerular neuron specification in the adult olfactory bulb. J. Neurosci. *28*, 6439–6452.

Brill, M.S., Ninkovic, J., Winpenny, E., Hodge, R.D., Ozen, I., Yang, R., Lepier, A., Gascon, S., Erdelyi, F., Szabo, G., et al. (2009). Adult generation of glutamatergic olfactory bulb interneurons. Nat. Neurosci. *12*, 1524–1533.

Casciola-Rosen, L., Rosen, A., Petri, M., and Schlissel, M. (1996). Surface blebs on apoptotic cells are sites of enhanced procoagulant activity: implications for coagulation events and antigenic spread in systemic lupus erythematosus. Proc. Natl. Acad. Sci. USA *93*, 1624–1629.

Chang, L.K., and Johnson, E.M., Jr. (2002). Cyclosporin A inhibits caspase-independent death of NGF-deprived sympathetic neurons: a potential role for mitochondrial permeability transition. J. Cell Biol. *157*, 771–781.

Chauhan, B.K., Reed, N.A., Zhang, W., Duncan, M.K., Kilimann, M.W., and Cvekl, A. (2002). Identification of genes downstream of Pax6 in the mouse lens using cDNA microarrays. J. Biol. Chem. *277*, 11539–11548.

Chen, J., Nagayama, T., Jin, K., Stetler, R.A., Zhu, R.L., Graham, S.H., and Simon, R.P. (1998). Induction of caspase-3-like protease may mediate delayed neuronal death in the hippocampus after transient cerebral ischemia. J. Neurosci. *18*, 4914–4928.

Conradt, B. (2009). Genetic control of programmed cell death during animal development. Annu. Rev. Genet. *43*, 493–523.

Costa, M.R., Wen, G., Lepier, A., Schroeder, T., and Götz, M. (2008). Par-complex proteins promote proliferative progenitor divisions in the developing mouse cerebral cortex. Development *135*, 11–22.

Cuddapah, S., Barski, A., Cui, K., Schones, D.E., Wang, Z., Wei, G., and Zhao, K. (2009). Native chromatin preparation and Illumina/Solexa library construction. Cold Spring Harb. Protoc. *2009*. 10.1101/pdb prot5237.

Cvekl, A., and Duncan, M.K. (2007). Genetic and epigenetic mechanisms of gene regulation during lens development. Prog. Retin. Eye Res. *26*, 555–597.

Cvekl, A., Sax, C.M., Bresnick, E.H., and Piatigorsky, J. (1994). A complex array of positive and negative elements regulates the chicken alpha A-crystallin gene: involvement of Pax-6, USF, CREB and/or CREM, and AP-1 proteins. Mol. Cell. Biol. *14*, 7363–7376.

Dicou, E., and Perez-Polo, J.R. (2009). Bax-an emerging role in ectopic cell death. Int. J. Dev. Neurosci. *27*, 299–304.

Dignam, J.D., Lebovitz, R.M., and Roeder, R.G. (1983). Accurate transcription initiation by RNA polymerase II in a soluble extract from isolated mammalian nuclei. Nucleic Acids Res. *11*, 1475–1489.

Eilken, H.M., Nishikawa, S., and Schroeder, T. (2009). Continuous single-cell imaging of blood generation from haemogenic endothelium. Nature *457*, 896–900.

Ellison-Wright, Z., Heyman, I., Frampton, I., Rubia, K., Chitnis, X., Ellison-Wright, I., Williams, S.C., Suckling, J., Simmons, A., and Bullmore, E. (2004). Heterozygous PAX6 mutation, adult brain structure and fronto-striato-thalamic function in a human family. Eur. J. Neurosci. *19*, 1505–1512.

Epstein, J.A., Glaser, T., Cai, J., Jepeal, L., Walton, D.S., and Maas, R.L. (1994). Two independent and interactive DNA-binding subdomains of the Pax6 paired domain are regulated by alternative splicing. Genes Dev. *8*, 2022–2034.

Ericson, J., Rashbass, P., Schedl, A., Brenner-Morton, S., Kawakami, A., van Heyningen, V., Jessell, T.M., and Briscoe, J. (1997). Pax6 controls progenitor cell identity and neuronal fate in response to graded Shh signaling. Cell *90*, 169–180.

Estivill-Torrus, G., Pearson, H., van Heyningen, V., Price, D.J., and Rashbass, P. (2002). Pax6 is required to regulate the cell cycle and the rate of progression from symmetrical to asymmetrical division in mammalian cortical progenitors. Development *129*, 455–466.

Favor, J., Peters, H., Hermann, T., Schmahl, W., Chatterjee, B., Neuhäuser-Klaus, A., and Sandulache, R. (2001). Molecular characterization of Pax6 (2Neu) through Pax6(10Neu): An extension of the Pax6 allelic series and the identification of two possible hypomorph alleles in the mouse Mus musculus. Genetics *159*, 1689–1700.

Favor, J., Gloeckner, C.J., Neuhäuser-Klaus, A., Pretsch, W., Sandulache, R., Saule, S., and Zaus, I. (2008). Relationship of Pax6 activity levels to the extent of eye development in the mouse, Mus musculus. Genetics *179*, 1345–1355.

Friedlander, R.M. (2003). Apoptosis and caspases in neurodegenerative diseases. N. Engl. J. Med. *348*, 1365–1375.

Ganguly, K., Favor, J., Neuhäuser-Klaus, A., Sandulache, R., Puk, O., Beckers, J., Horsch, M., Schädler, S., Vogt Weisenhorn, D., Wurst, W., and Graw, J. (2008). Novel allele of crybb2 in the mouse and its expression in the brain. Invest. Ophthalmol. Vis. Sci. *49*, 1533–1541.

Glaser, T., Walton, D.S., and Maas, R.L. (1992). Genomic structure, evolutionary conservation and aniridia mutations in the human PAX6 gene. Nat. Genet. *2*, 232–239.

Götz, M., Stoykova, A., and Gruss, P. (1998). Pax6 controls radial glia differentiation in the cerebral cortex. Neuron *21*, 1031–1044.

Graw, J. (2009). Genetics of crystallins: Cataract and beyond. Exp. Eye Res. *88*, 173–189.

Graw, J., Löster, J., Puk, O., Münster, D., Haubst, N., Soewarto, D., Fuchs, H., Meyer, B., Nürnberg, P., Pretsch, W., et al. (2005). Three novel Pax6 alleles in the mouse leading to the same small-eye phenotype caused by different consequences at target promoters. Invest. Ophthalmol. Vis. Sci. *46*, 4671–4683.

Hack, M.A., Saghatelyan, A., de Chevigny, A., Pfeifer, A., Ashery-Padan, R., Lledo, P.M., and Götz, M. (2005). Neuronal fate determinants of adult olfactory bulb neurogenesis. Nat. Neurosci. *8*, 865–872.

Hatzold, J., and Conradt, B. (2008). Control of apoptosis by asymmetric cell division. PLoS Biol. *6*, e84. 10.1371/journal.pbio.0060084.

Haubst, N., Berger, J., Radjendirane, V., Graw, J., Favor, J., Saunders, G.F., Stoykova, A., and Götz, M. (2004). Molecular dissection of Pax6 function: The specific roles of the paired domain and homeodomain in brain development. Development *131*, 6131–6140.

Heins, N., Malatesta, P., Cecconi, F., Nakafuku, M., Tucker, K.L., Hack, M.A., Chapouton, P., Barde, Y.A., and Götz, M. (2002). Glial cells generate neurons: the role of the transcription factor Pax6. Nat. Neurosci. *5*, 308–315.

Hirsch, E.C., Graybiel, A.M., Duyckaerts, C., and Javoy-Agid, F. (1987). Neuronal loss in the pedunculopontine tegmental nucleus in Parkinson disease and in progressive supranuclear palsy. Proc. Natl. Acad. Sci. USA *84*, 5976–5980.

Holm, P.C., Mader, M.T., Haubst, N., Wizenmann, A., Sigvardsson, M., and Götz, M. (2007). Loss- and gain-of-function analyses reveal targets of Pax6 in the developing mouse telencephalon. Mol. Cell. Neurosci. *34*, 99–119.

Kamradt, M.C., Chen, F., and Cryns, V.L. (2001). The small heat shock protein alpha B-crystallin negatively regulates cytochrome c- and caspase-8-dependent activation of caspase-3 by inhibiting its autoproteolytic maturation. J. Biol. Chem. *276*, 16059–16063.

Kohwi, M., Osumi, N., Rubenstein, J.L., and Alvarez-Buylla, A. (2005). Pax6 is required for making specific subpopulations of granule and periglomerular neurons in the olfactory bulb. J. Neurosci. *25*, 6997–7003.

Kosaka, K., and Kosaka, T. (2007). Chemical properties of type 1 and type 2 periglomerular cells in the mouse olfactory bulb are different from those in the rat olfactory bulb. Brain Res. *1167*, 42–55.

Kosaka, K., Hama, K., Nagatsu, I., Wu, J.Y., and Kosaka, T. (1988). Possible coexistence of amino acid (gamma-aminobutyric acid), amine (dopamine) and peptide (substance P); neurons containing immunoreactivities for glutamic acid decarboxylase, tyrosine hydroxylase and substance P in the hamster main olfactory bulb. Exp. Brain Res. *71*, 633–642.

Kroll, T.T., and O'Leary, D.D. (2005). Ventralized dorsal telencephalic progenitors in Pax6 mutant mice generate GABA interneurons of a lateral ganglionic eminence fate. Proc. Natl. Acad. Sci. USA *102*, 7374–7379.

Lagace, D.C., Whitman, M.C., Noonan, M.A., Ables, J.L., DeCarolis, N.A., Arguello, A.A., Donovan, M.H., Fischer, S.J., Farnbauch, L.A., Beech, R.D., et al. (2007). Dynamic contribution of nestin-expressing stem cells to adult neurogenesis. J. Neurosci. *27*, 12623–12629.

Lanneau, D., Brunet, M., Frisan, E., Solary, E., Fontenay, M., and Garrido, C. (2008). Heat shock proteins: Essential proteins for apoptosis regulation. J. Cell. Mol. Med. *12*, 743–761.

Lee, T.I., Johnstone, S.E., and Young, R.A. (2006). Chromatin immunoprecipitation and microarray-based analysis of protein location. Nat. Protoc. *1*, 729–748.

Liang, G., Lin, J.C.Y., Wei, V., Yoo, C., Cheng, J.C., Nguyen, C.T., Weisenberger, D.J., Egger, G., Takai, D., Gonzales, F.A., and Jones, P.A. (2004). Distinct localization of histone H3 acetylation and H3-K4 methylation to the transcription start sites in the human genome. Proc. Natl. Acad. Sci. USA *101*, 7357–7362.

Lois, C., and Alvarez-Buylla, A. (1994). Long-distance neuronal migration in the adult mammalian brain. Science *264*, 1145–1148.

Magabo, K.S., Horwitz, J., Piatigorsky, J., and Kantorow, M. (2000). Expression of betaB(2)-crystallin mRNA and protein in retina, brain, and testis. Invest. Ophthalmol. Vis. Sci. *41*, 3056–3060.

Mao, Y.W., Liu, J.P., Xiang, H., and Li, D.W. (2004). Human alphaA- and alphaB-crystallins bind to Bax and Bcl-X(S) to sequester their translocation during staurosporine-induced apoptosis. Cell Death Differ. *11*, 512–526.

Morozov, V., and Wawrousek, E.F. (2006). Caspase-dependent secondary lens fiber cell disintegration in alphaA-/alphaB-crystallin double-knockout mice. Development *133*, 813–821.

Nakamura, K., Hioki, H., Fujiyama, F., and Kaneko, T. (2005). Postnatal changes of vesicular glutamate transporter (VGluT)1 and VGluT2 immunoreactivities and their colocalization in the mouse forebrain. J. Comp. Neurol. *492*, 263–288.

Narayanan, S., Kamps, B., Boelens, W.C., and Reif, B. (2006). alphaB-crystallin competes with Alzheimer's disease beta-amyloid peptide for peptide-peptide interactions and induces oxidation of Abeta-Met35. FEBS Lett. *580*, 5941–5946.

Nikoletopoulou, V., Plachta, N., Allen, N.D., Pinto, L., Götz, M., and Barde, Y.A. (2007). Neurotrophin receptor-mediated death of misspecified neurons generated from embryonic stem cells lacking Pax6. Cell Stem Cell *1*, 529–540.

Ninkovic, J., Mori, T., and Götz, M. (2007). Distinct modes of neuron addition in adult mouse neurogenesis. J. Neurosci. *27*, 10906–10911.

Novak, A., Guo, C., Yang, W., Nagy, A., and Lobe, C.G. (2000). Z/EG, a double reporter mouse line that expresses enhanced green fluorescent protein upon Cre-mediated excision. Genesis *28*, 147–155.

Osumi, N., Shinohara, H., Numayama-Tsuruta, K., and Maekawa, M. (2008). Concise review: Pax6 transcription factor contributes to both embryonic and adult neurogenesis as a multifunctional regulator. Stem Cells *26*, 1663–1672.

Petreanu, L., and Alvarez-Buylla, A. (2002). Maturation and death of adult-born olfactory bulb granule neurons: role of olfaction. J. Neurosci. *22*, 6106–6113.

Plachta, N., Annaheim, C., Bissière, S., Lin, S., Rüegg, M., Hoving, S., Müller, D., Poirier, F., Bibel, M., and Barde, Y.A. (2007). Identification of a lectin causing the degeneration of neuronal processes using engineered embryonic stem cells. Nat. Neurosci. *10*, 712–719.

Rekas, A., Adda, C.G., Andrew Aquilina, J., Barnham, K.J., Sunde, M., Galatis, D., Williamson, N.A., Masters, C.L., Anders, R.F., Robinson, C.V., et al. (2004). Interaction of the molecular chaperone alphaB-crystallin with alpha-synuclein: effects on amyloid fibril formation and chaperone activity. J. Mol. Biol. *340*, 1167–1183.

Renkawek, K., de Jong, W.W., Merck, K.B., Frenken, C.W., van Workum, F.P., and Bosman, G.J. (1992). alpha B-crystallin is present in reactive glia in Creutzfeldt-Jakob disease. Acta Neuropathol. *83*, 324–327.

Revay, R., Vaughan, R., Grant, S., and Kuhar, M.J. (1996). Dopamine transporter immunohistochemistry in median eminence, amygdala, and other areas of the rat brain. Synapse *22*, 93–99.

Schuurmans, C., and Guillemot, F. (2002). Molecular mechanisms underlying cell fate specification in the developing telencephalon. Curr. Opin. Neurobiol. *12*, 26–34.

Shih, M.C., Franco de Andrade, L.A., Amaro, E., Jr., Felicio, A.C., Ferraz, H.B., Wagner, J., Hoexter, M.Q., Lin, L.F., Fu, Y.K., Mari, J.J., et al. (2007). Higher nigrostriatal dopamine neuron loss in early than late onset Parkinson's disease?—a [99mTc]-TRODAT-1 SPECT study. Mov. Disord. *22*, 863–866.

Staines, W.A., Morassutti, D.J., Reuhl, K.R., Ally, A.I., and McBurney, M.W. (1994). Neurons derived from P19 embryonal carcinoma cells have varied morphologies and neurotransmitters. Neuroscience *58*, 735–751.

Stoykova, A., and Gruss, P. (1994). Roles of Pax-genes in developing and adult brain as suggested by expression patterns. J. Neurosci. *14*, 1395–1412.

Stoykova, A., Treichel, D., Hallonet, M., and Gruss, P. (2000). Pax6 modulates the dorsoventral patterning of the mammalian telencephalon. J. Neurosci. *20*, 8042–8050.

Sulzer, D. (2007). Multiple hit hypotheses for dopamine neuron loss in Parkinson's disease. Trends Neurosci. *30*, 244–250.

Toresson, H., Potter, S.S., and Campbell, K. (2000). Genetic control of dorsal-ventral identity in the telencephalon: Opposing roles for Pax6 and Gsh2. Development *127*, 4361–4371.

Tuoc, T.C., and Stoykova, A. (2008). Trim11 modulates the function of neurogenic transcription factor Pax6 through ubiquitin-proteosome system. Genes Dev. *22*, 1972–1986.

Tuoc, T.C., Radyushkin, K., Tonchev, A.B., Piñon, M.C., Ashery-Padan, R., Molnár, Z., Davidoff, M.S., and Stoykova, A. (2009). Selective cortical layering abnormalities and behavioral deficits in cortex-specific Pax6 knock-out mice. J. Neurosci. *29*, 8335–8349.

Wiznerowicz, M., and Trono, D. (2003). Conditional suppression of cellular genes: Lentivirus vector-mediated drug-inducible RNA interference. J. Virol. *77*, 8957–8961.

Wolf, L.V., Yang, Y., Wang, J., Xie, Q., Braunger, B., Tamm, E.R., Zavadil, J., and Cvekl, A. (2009). Identification of pax6-dependent gene regulatory networks in the mouse lens. PLoS ONE *4*, e4159. 10.1371/journal.pone.0004159.

Xi, J.H., Bai, F., Gross, J., Townsend, R.R., Menko, A.S., and Andley, U.P. (2008). Mechanism of small heat shock protein function in vivo: A knock-in mouse model demonstrates that the R49C mutation in alpha A-crystallin enhances protein insolubility and cell death. J. Biol. Chem. *283*, 5801–5814.

Yang, Y., Stopka, T., Golestaneh, N., Wang, Y., Wu, K., Li, A., Chauhan, B.K., Gao, C.Y., Cveklová, K., Duncan, M.K., et al. (2006). Regulation of alphaA-crystallin via Pax6, c-Maf, CREB and a broad domain of lens-specific chromatin. EMBO J. *25*, 2107–2118.

Yun, K., Potter, S., and Rubenstein, J.L. (2001). Gsh2 and Pax6 play complementary roles in dorsoventral patterning of the mammalian telencephalon. Development *128*, 193–205.

Zhao, C., Deng, W., and Gage, F.H. (2008). Mechanisms and functional implications of adult neurogenesis. Cell *132*, 645–660.

Zhuang, X., Masson, J., Gingrich, J.A., Rayport, S., and Hen, R. (2005). Targeted gene expression in dopamine and serotonin neurons of the mouse brain. J. Neurosci. Methods *143*, 27–32.